Fine Tactile Manipulation via Force-Guided Vision-Free Controller for Peg Insertion and Disengagement

by

Soibkhon Khajikhanov

Submitted to the Department of Robotics and Mechatronics
in partial fulfillment of the requirements for the degree of

Master of Science in Robotics

at the

NAZARBAYEV UNIVERSITY

April 2025

Author .....
Department of Robotics and Mechatronics
April 15, 2025

Certified by .....
Zhanat Kappassov
Associate Professor
Thesis Supervisor

Accepted by .....
Elizabeth Arkhangelsky
Dean, School of Engineering and Digital Sciences

Fine Tactile Manipulation via Force-Guided Vision-Free Controller for Peg Insertion and Disengagement

by

Soibkhon Khajikhanov

Submitted to the Department of Robotics and Mechatronics
on April 15, 2025, in partial fulfillment of the
requirements for the degree of
Master of Science in Robotics

Abstract

Executing the Peg-In-Hole operation in variable environments continues to pose a challenge for autonomous robots. Most popular way of solving this task is typically via visual feedback. However, alternative sensing methods are critical in environments where visual data is limited or unreliable, and in the case of occlusion by end-effector. This paper presents a novel force-guided vision-free controller fitted for fine tactile manipulation, specifically peg insertion and extraction tasks using a USB stick. By utilizing force feedback, the controller operates without visual input, relying solely on tactile sensing for precise manipulation. The system processes real-time force and torque data from the manipulator to guide the peg's alignment and establish initial insertion into a hole. To enable further fine insertion tactile feedback is used. Specifically, we focus on manipulating the peg with a parallel gripper integrated with a tactile sensor. The sensor data is processed to track in-hand rotations of the peg's pose, which is then fed back to the robot controller. This feedback enables the system to compensate for variations in peg orientation and end-point position during task execution. After successful insertion, the wiggle movement is initiated via force control to extract the peg. The proposed approach is validated on the Franka Emika manipulator using a two-finger Robotiq 2F-85 gripper equipped with Xela capacitive-based tactile sensor arrays, each containing 16 tactile elements.

Thesis Supervisor: Zhanat Kappassov
Title: Associate Professor

Contents

List of Figures

List of Tables

Chapter 1

Introduction

Peg insertion is a classic problem in robotics, often used to evaluate a robot's manipulation capabilities. It involves aligning a peg with a hole and inserting it, requiring precise positioning and orientation. Traditionally, this task relies on visual feedback, where cameras or vision systems guide the robot to align the peg before using force feedback for the final insertion [1]. However, in environments where visual information is unavailable or unreliable—such as dark settings, underwater, or cluttered spaces—robots must rely on alternative sensory modalities, specifically force and tactile sensing [2]. Thus this task can be divided into contact model-based control and contact model-free [3].

The thesis focuses on a vision-free approach, where the robot performs peg insertion using only force and tactile data [4]. This is significant because it expands the robot's operational range to scenarios where vision is impractical, such as in space exploration [5], underwater operations, or manufacturing areas with poor lighting. The motivation lies in enhancing robot robustness and efficiency, enabling them to handle tasks in diverse and challenging conditions [6].

1.1 Background and Motivation

In conventional robotic peg insertion, visual feedback is used to initially align the peg with the hole, and force feedback ensures the insertion is completed without

jamming [1] or damage. However, in vision-free scenarios, the robot must rely solely on force and tactile sensing to both locate the hole and guide the insertion [2, 4]. This introduces several challenges:

Position Uncertainty: The robot starts without knowing the hole's location, requiring a search strategy based on force feedback [3].

Contact State Identification: The robot must interpret force and torque measurements to determine its state, such as being in free space, touching the surface, or aligned with the hole [7].

Force Control: Applying appropriate forces is crucial to avoid damaging the peg, hole, or robot, while ensuring successful insertion [8].

Tactile sensing plays a pivotal role here. While force/torque sensors measure overall forces and torques at the end effector, advanced tactile sensors provide detailed spatial information about the contact area, such as pressure distribution or contact shape [6]. This finer-grained data is essential for accurate alignment and insertion, especially without visual cues. For instance, tactile sensors can help detect the orientation of the peg relative to the hole, aiding in fine-tuning during the insertion process [2].

1.2 Peg-in-hole methods

A wide range of scholars and industry experts have concentrated their efforts on enhancing robotic peg-in-hole assembly techniques, leveraging diverse learning frameworks. These include classical conditioning through established compliant control methods [9], observational learning via demonstration-based approaches [10], and operant conditioning through environmental interactions [11]. In this thesis, we classify the current strategies for peg-in-hole assembly into two broad categories: those reliant on contact models and those that operate without them. Within the contact model-free category, we further distinguish between strategies based on learning from demonstrations and those based on learning from environmental feedback.

1.2.1 Contact model based

Contact model-based strategies analyze contact interactions to guide robotic peg-in-hole assembly. These approaches typically involve identifying contact states using friction and contact dynamics [12], followed by applying preprogrammed compliant control tailored to those states. They are highly effective for high-precision tasks [13, 14, 15] and large-scale assemblies [16, 17, 18], especially with limited sensor data. Research has addressed complex scenarios like multi-peg-in-hole setups [19, 20, 21], though it often optimizes contact-state recognition [22, 23] and control execution [24, 25] independently. This separation highlights a research gap: integrating these stages could enhance performance [12]. These strategies thrive in structured environments where contact dynamics are predictable, but their reliance on predefined models may reduce flexibility in dynamic settings.

1.2.2 Contact model free

Contact model-free strategies, such as Learning from Demonstrations (LFD) [26, 18, 27, 28] and Learning from Environments (LFE) [29], avoid explicit contact modeling. LFD trains robots by replicating human demonstrations [30, 31], excelling in unstructured environments but lacking generalization. LFE, often employing Reinforcement Learning (RL) [32, 33], learns through trial-and-error interactions [14, 34], though it requires substantial data. Recent progress integrates RL with demonstrations or prior knowledge for efficiency [20, 35, 15], while model-based RL uses transition dynamics to guide learning [33, 36]. These methods offer adaptability without needing detailed contact models. However, combining them with traditional contact-based approaches remains underexplored, presenting potential to improve robustness in robotic assembly.

1.2.3 Problem statement

Most existing research primarily focuses on peg insertion in low or frictionless environments. However, in industrial settings, instances of high friction between the peg

and the hole are more common, necessitating more precise force control and tactile sensing to successfully complete the insertion process. This thesis addresses the insertion of a USB stick into a port, a task where friction plays a significant role. It is well-established that the insertion of a USB stick typically encounters resistance due to friction, which impacts the force dynamics during the operation. Additionally, this work also explores the disengagement of the peg (i.e., unplugging). While disengagement is generally not a challenging task in the absence of friction, in the presence of friction, more refined manipulator control is required to ensure proper disengagement and verify that the peg has been fully unplugged.

Chapter 2

Literature review

Peg-in-hole (PiH) assembly represents a fundamental challenge in robotic manipulation and has been extensively studied in the robotics research community. Various approaches have been proposed to address this task, with significant differences in sensing modalities and control strategies. A common approach to PiH assembly utilizes force/torque (F/T) sensors mounted on the robot wrist to detect contact forces during insertion [37, 38, 39, 40, 41]. These methods rely on sensing the interaction forces between the peg and hole to guide the insertion process. However, as noted by several researchers, F/T sensors increase system costs and require high control frequencies [42]. Alternative methods focus on analyzing contact states using sensors at the robot joints [43, 44, 45]. These approaches are typically designed for specific peg geometries and are often combined with compliant control strategies to compensate for inaccuracies in hole center estimation. Most existing research assumes the peg is rigidly attached to the robot end-effector, eliminating uncertainty in the peg's pose [42]. However, this creates limitations for multi-operation assembly tasks where a single gripper would be more practical. When the peg is held by a gripper rather than rigidly attached, external forces during insertion can change the peg's in-hand pose, significantly increasing task complexity. Recent work has begun exploring PiH assembly with grippers and dexterous hands [46, 47]. Kim and Rodriguez [46] used high-resolution tactile sensors with a parallel gripper, relying on friction from the sensor's compliant layer to maintain a stable grasp. Other researchers have implemented

compliant-controlled robot hands with force feedback from load cells embedded in the fingertips [47]. However, these approaches typically don't directly address detection and compensation for large variations in the peg's in-hand pose during insertion. Tactile sensing shows promising potential for addressing these challenges, as it has proven effective for in-hand object pose estimation [48, 49] and contact localization [50, 51]. These capabilities could enable more robust PiH assembly with grippers by providing continuous feedback about the peg's position and orientation during the insertion process.

Moreover, hybrid control methods combining force control with visual or tactile sensing have been proposed to enhance robustness [52, 53]. Vision-based strategies can provide global guidance, while tactile feedback refines alignment at finer scales [54]. The use of capacitive-based tactile sensors, such as those employed in our research, has been shown to provide high-resolution force distribution information that can be leveraged for precise in-hand manipulation [55].

In summary, PiH research has evolved from traditional force-based methods to more advanced tactile and learning-driven strategies. However, challenges remain in achieving robust in-hand pose estimation and adaptive control in variable environments. Our work builds upon these advancements by integrating real-time tactile feedback into a force-guided vision-free PiH controller, addressing the limitations of prior methods and enabling robust manipulation in visually constrained settings.

Chapter 3

Methodology

3.1 Vision-free based control

First, the manipulator is given an approximate location of the hole rather than an exact position. Since the precise hole position is unknown, the manipulator must perform an exploratory sliding motion along the surface to locate it. This exploration phase ensures that the peg makes continuous contact with the surface, allowing the system to detect changes in force and position that indicate the hole's presence.

Once the hole is identified, the process transitions to the second phase of insertion. At this stage, tactile feedback from the sensor-equipped manipulator is utilized to carefully guide the peg into the hole, ensuring precise alignment and minimizing insertion forces. This step is crucial for preventing jamming or misalignment, which could compromise the success of the task.

3.2 Assebly strategy

To enhance the effectiveness of the insertion process, the manipulator executes a controlled sinusoidal motion. This oscillatory movement helps in overcoming friction and aligning the peg dynamically, improving the success rate of insertion. The sinusoidal motion pattern, as illustrated in 3-1, ensures smooth guidance and facilitates the peg's entry into the hole.

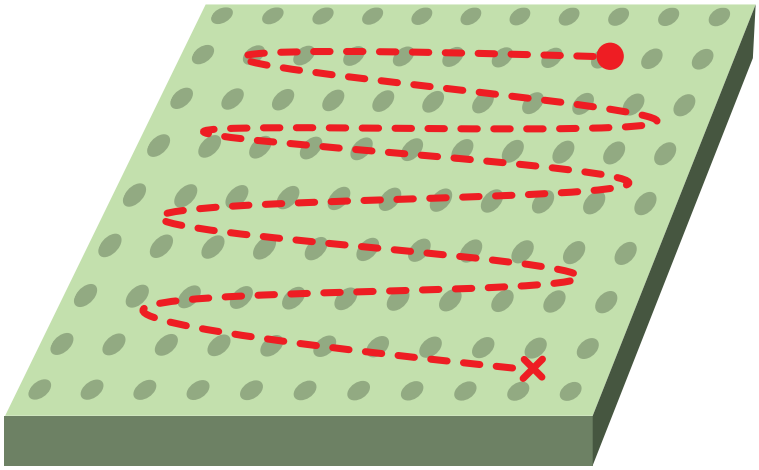

Figure 3-1: Algorithm to search for the hole

After the location of the hole is found the next step of the insertion is initiated. In this step the Xela 4x4 tactile sensor is used to generate force vector data to further align the peg into the hole. The sensor is mounted on only one side of the gripper, as this thesis aims to develop a cost-effective solution for the peg-in-hole problem. By utilizing a single sensor, the system minimizes hardware expenses while still enabling effective tactile feedback for guiding the insertion process. This approach balances affordability and functionality, demonstrating that precise peg insertion can be achieved without the need for multiple expensive sensors. The steps for the tactile insertion is demonstrated in 3-2

It is common knowledge that a USB stick to not enter the hole with one right motion, the wiggle is needed, thus as illustrated in the last step, the manipulator moves the peg side-to-side while making sure that it is entering the hole.

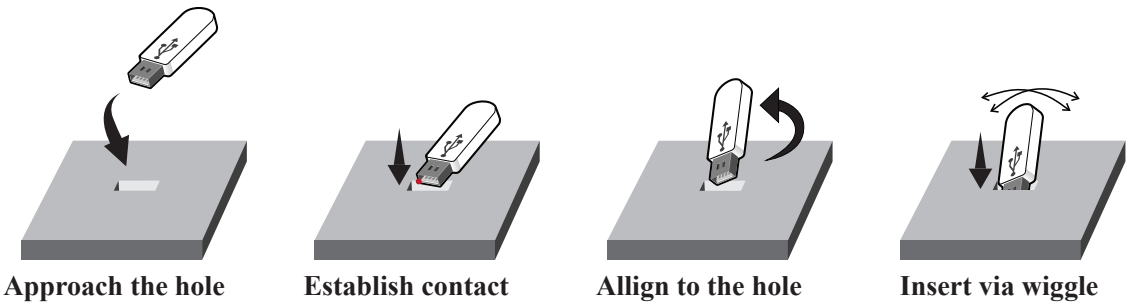

Figure 3-2: Algorithm to search for the hole

3.3 Setup

The Franka Emika manipulator was selected for this research due to its advanced torque-sensing capabilities at each joint, making it particularly suitable for force-controlled tasks. The control scheme implemented in this study integrates both force control and impedance control to achieve robust performance during the peg-in-hole insertion task.

3.3.1 Force Control Implementation

Force control is essential for maintaining consistent contact between the peg and the surface during the exploration phase. The Franka Emika's control architecture allows for direct force control in Cartesian space, where the desired force vector $\mathbf{F_d}$ is set perpendicular to the surface plane. The force controller can be represented as:

$$\tau = \mathbf{J}^T(K_p(\mathbf{F_d} - \mathbf{F_m}) + K_i \int (\mathbf{F_d} - \mathbf{F_m})dt) \tag{3.1}$$

where τ represents the joint torques, $\mathbf{J}$ is the manipulator Jacobian, K_p and K_i are proportional and integral gains respectively, and $\mathbf{F_m}$ is the measured force from the end-effector. This control scheme ensures that the peg maintains consistent contact with the surface without applying excessive force that might damage either the peg or the surface.

During the exploration phase, a force threshold of $5N$ was established to prevent

damage while ensuring sufficient contact. The force controller was tuned to respond quickly to changes in surface topology, particularly when the edge of the hole is encountered.

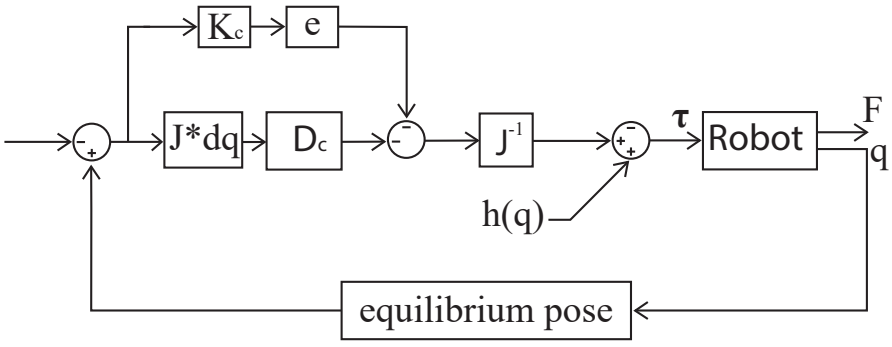

Figure 3-3: Block diagram of the manipulator control

3.3.2 Impedance Control for Insertion

Once the hole is located, the control scheme transitions to impedance control, which models the manipulator behavior as a mass-spring-damper system. This approach is particularly effective for insertion tasks as it allows for compliant motion while maintaining position accuracy. The impedance controller can be described as:

$$\mathbf{M}(\mathbf{q})\ddot{\mathbf{x}} + \mathbf{D}(\mathbf{q})\dot{\mathbf{x}} + \mathbf{K}(\mathbf{q})(\mathbf{x} - \mathbf{x_d}) = \mathbf{F_{ext}} \tag{3.2}$$

where $\mathbf{M}(\mathbf{q})$, $\mathbf{D}(\mathbf{q})$, and $\mathbf{K}(\mathbf{q})$ are the inertia, damping, and stiffness matrices respectively, $\mathbf{x}$ is the current position, $\mathbf{x_d}$ is the desired position, and $\mathbf{F_{ext}}$ is the external force acting on the manipulator.

The impedance parameters were carefully tuned to ensure that the manipulator could respond appropriately to contact forces during insertion. Lower stiffness values ($K = 800N/m$ in the x and y directions, and $K = 1200N/m$ in the z direction) were chosen to allow for compliance in the lateral directions while maintaining sufficient stiffness in the insertion direction.

3.3.3 Hybrid Control Strategy

A hybrid control strategy was implemented to combine the benefits of both force and impedance control. During the sinusoidal search motion, impedance control was used in the lateral directions (x and y) while force control was maintained in the vertical direction (z). This hybrid approach allowed for precise control of the contact force while permitting compliant motion in the search plane.

The sinusoidal search pattern was generated using the following equations:

$$x(t) = A_x \sin(\omega_x t) \tag{3.3}$$

$$y(t) = A_y \sin(\omega_y t + \phi) \tag{3.4}$$

where A_x and A_y are the amplitudes of the motion in the x and y directions, ω_x and ω_y are the frequencies, and ϕ is the phase difference between the x and y motions. The amplitudes were set to decrease gradually as the peg approached the hole, based on the feedback from the tactile sensor.

3.3.4 Adaptive Control Components

To enhance the system's robustness to variations in hole position and orientation, adaptive control elements were incorporated. The system continuously updated the estimated hole position based on the tactile feedback and adjusted the control parameters accordingly. This adaptive approach was particularly valuable when dealing with holes that were not perfectly perpendicular to the surface.

The adaptation law for the impedance parameters can be expressed as:

$$\dot{\mathbf{K}} = -\Gamma \cdot \mathbf{e} \cdot \dot{\mathbf{x}}^T \tag{3.5}$$

where Γ is a positive definite adaptation gain matrix, $\mathbf{e}$ is the position error, and $\dot{\mathbf{x}}$ is the end-effector velocity.

3.3.5 Tactile Feedback Integration

The Xela 4×4 tactile sensor provided crucial feedback for the insertion phase. The sensor data was processed to extract the force distribution across the sensor array, which was then used to calculate the principal direction of force. This information guided the alignment of the peg with the hole.

The force vector data from the tactile sensor was filtered using a low-pass filter to reduce noise and then transformed into the manipulator's base frame. The resulting force vector was used to modify the impedance control parameters, particularly the stiffness in the direction of the detected force.

Through this comprehensive control strategy, the Franka Emika manipulator was able to successfully locate and insert pegs into holes with varying positions and orientations, demonstrating the effectiveness of the proposed methodology for vision-free peg-in-hole assembly tasks.

Chapter 4

Implementation and System Architecture

This chapter details the practical implementation of the control methodologies outlined in Chapter 2. The focus is on translating theoretical control approaches into a functional system capable of performing vision-free peg-in-hole insertions using the Franka Emika manipulator.

4.1 Hardware Setup

4.1.1 Franka Emika Manipulator Configuration

The Franka Emika Panda robot was configured with its standard 7 degrees of freedom (DOF) setup. The manipulator was mounted on a stable base to ensure consistent performance during the insertion tasks. For this implementation, the following hardware specifications were utilized:

- Joint torque sensors with a resolution of 0.1 Nm
- End-effector payload capacity of 3 kg
- Joint position accuracy of ± 0.1 mm
- Control frequency of 1 kHz

The robot's end-effector was equipped with a Robotiq 2F-85 gripper with a tactile sensor attached to one finger.

4.1.2 Tactile Sensing System

The Xela 4×4 tactile sensor was integrated onto one side of the gripper as described in the methodology. The sensor provides a 16-element (4×4) array of 3-axis force measurements. Each sensing element outputs force vectors in local x, y, and z directions, providing comprehensive tactile feedback during the insertion process.

The sensor was connected to the control system via USB interface, with data acquisition performed at 100 Hz. This sampling rate proved sufficient for detecting the subtle force changes that occur during contact with the hole edge.

4.1.3 Test Environment

A standardized test environment was constructed to evaluate the insertion strategy. This consisted of:

- A flat plastic plate (150 mm $\times$150 mm $\times$10 mm) with USB hole
- USB sticks (pegs)
- An adjustable mounting system allowing for controlled variation of hole positions and orientations

4.2 Software Architecture

4.2.1 Control System Integration

The control system was implemented using ROS (Robot Operating System) Noetic running on Ubuntu 20.04. The `libfranka` C++ library provided low-level access to the Franka Control Interface (FCI), enabling direct torque control at the required 1 kHz frequency.

The overall software architecture follows a modular design with the following key components:

- **State Machine**: Manages the transition between exploration and insertion phases
- **Force Controller**: Implements the force control algorithm described in Section 2.1.3
- **Impedance Controller**: Implements the impedance control algorithm
- **Trajectory Generator**: Generates the sinusoidal search patterns
- **Tactile Data Processor**: Processes and interprets the tactile sensor data
- **Parameter Adapter**: Adjusts control parameters based on feedback

4.2.2 Algorithmic Implementation

The exploration strategy employed a sinusoidal trajectory across a $150\,\text{mm} \times 150\,\text{mm}$ plate, incorporating both lateral and vertical motions. The path was defined by:

$$x(t) = A\sin(\omega t), \quad y(t) = vt, \quad z(t) = z_0 + B\sin(\nu t)$$

where A is the horizontal amplitude of oscillation, ω is the lateral angular frequency, v is the constant forward scanning velocity along the y-axis, z_0 is the nominal height above the surface, B is the vertical amplitude, and ν is the vertical angular frequency. This sinusoidal pattern enabled efficient coverage of the surface area while maintaining periodic vertical motion, facilitating robust detection of the target feature during the scanning process.

The tactile data processing algorithm employed a weighted centroid approach to determine the principal direction of force:

$$\mathbf{F_{principal}} = \frac{\sum_{i=1}^{16} \|\mathbf{F_i}\| \cdot \mathbf{F_i}}{\sum_{i=1}^{16} \|\mathbf{F_i}\|} \tag{4.1}$$

where $\mathbf{F_i}$ represents the force vector from the i-th tactile element.

4.2.3 System Calibration

Prior to operation, a calibration routine was performed to establish:

- The relationship between the tactile sensor reference frame and the robot end-effector frame
- The force-to-voltage conversion factors for accurate force measurement
- Baseline (zero) values for the tactile sensor elements under no load

This calibration process ensured consistent performance across multiple experimental trials and reduced systematic errors in force measurement and control.

4.3 Experiment Design

The experimental evaluation of the system was structured to test the robustness of the implementation across varying conditions. The test parameters included:

- Hole position uncertainty: ± 10 mm in x, y directions
- Peg angular misalignment: $0°$, $15°$, and $30°$ approximately from vertical
- Different hole size: tight, moderate, and heavily used (meaning new (tight) or heavily used usb hole

For each parameter combination, 30 trials were conducted to ensure the statistical significance of the results. Success was defined as the complete insertion of the peg to the designated depth within a 60-second time limit.

4.4 Estimating the pose of the peg

Because the peg isn't rigidly fixed to the robot's gripper, interactions between the peg and either the hole or the surrounding environment can alter the peg's in-hand

pose. In this work, we assume that such external forces cause the peg to pivot around the center point between the two fingers, as illustrated in 4-1. We treat other types of motion as negligible, assuming that the grasping force and the friction from the compliant layer are sufficient to allow only minor shifts in the peg's position—similar to the assumptions made in [56, 8]. Within this framework, tactile sensing is used to estimate the peg's in-hand orientation $\theta \in R$ and the position of its tip $\mathbf{p} \in R^3$ (as defined in the finger's local frame in 4-1) at each time step. This information is then used to provide feedback for controlling the robot during the insertion process.

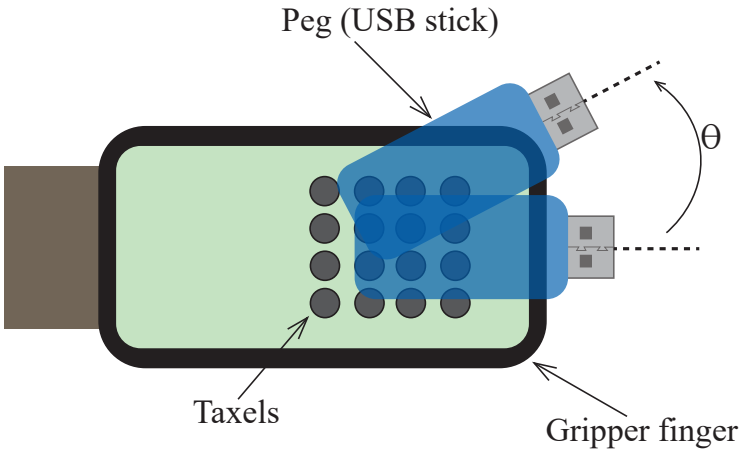

Figure 4-1: Representation of the peg in the gripper finger

Chapter 5

Experimental Results

This chapter presents the experimental results obtained from the implementation described in Chapter 4. The results evaluate the performance and robustness of the proposed control framework for vision-free peg-in-hole insertion using the Franka Emika Panda manipulator.

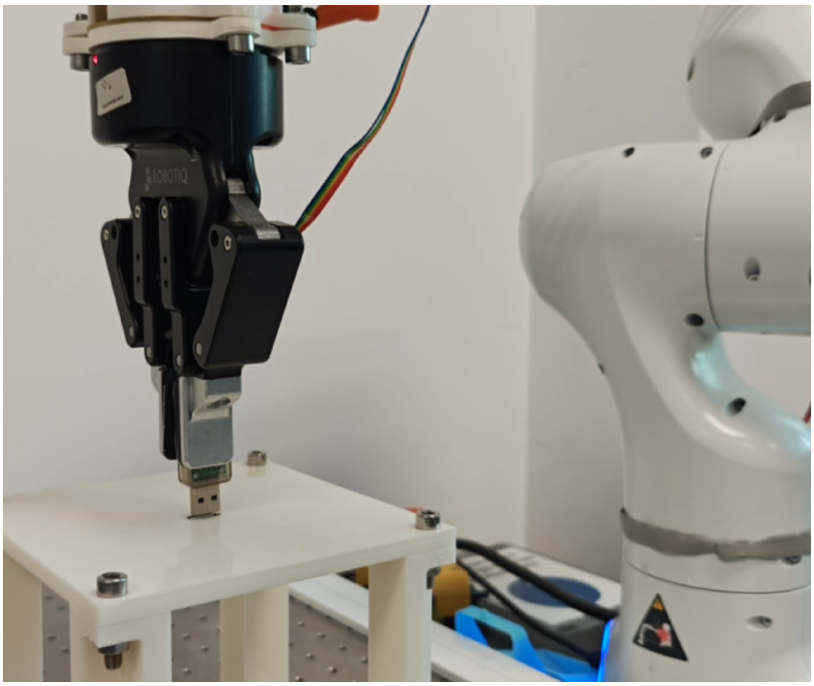

Figure 5-1: The setup with 15x15cm platform to hold USB hole

5.1 Overview

The experiments aimed to validate the ability of the robot to perform insertion tasks under varying uncertainties and conditions. Metrics such as success rate, insertion time, and pose estimation accuracy were used for evaluation. The experiments were repeated 30 times for each test condition to ensure statistical reliability.

5.2 Success Rates Across Conditions

5.2.1 Hole Position Uncertainty

To evaluate robustness against positional uncertainties, the peg's initial position was randomly shifted within a range of ±10 mm in both x and y directions. The average success rates under these perturbations are summarized in Table 5.1.

Table 5.1: Success rate under hole position uncertainty (±10 mm)

Displacement Range (mm)	**Success Rate (%)**
±5	86.6
±10	76.6

Changing of an initial position affected the success rate due to the peg falling out of the 150x150mm plate range since robot control was not modeled to compensate for the initial position as we are using force control, not position.

5.2.2 Angular Misalignment of the Peg

The peg was manually misaligned relative to the vertical axis by approximately 0°, 15°, and 30° to test the system's sensitivity to angular deviations. Table 5.2 presents the success rates.

Table 5.2: Success rate with varying angular misalignment

Angular Misalignment (deg)	**Success Rate**
0°	29/30
15°	27/30
30°	23/30

Performance degraded with increased misalignment, but the control system remained effective at correcting pose deviations up to 30°.

5.2.3 Hole Condition Variability

Insertions were tested across three hole conditions: tight (new), moderate (standard), and heavily used (worn).

Tight fits showed slightly lower performance due to increased contact forces, while heavily used holes had the highest success rate due to their compliance.

5.3 Insertion Time Analysis

The average insertion time for successful trials under each scenario is presented in Figure 5-2. The time includes only the insertion part of the experiment.

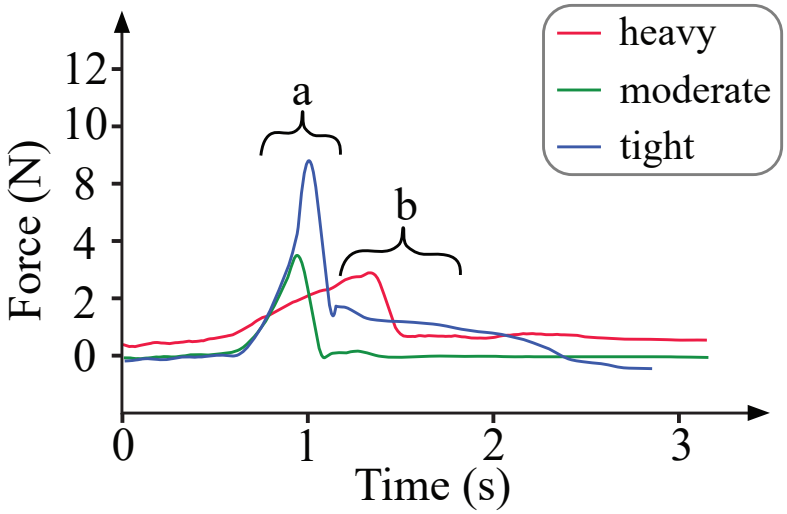

Figure 5-2: Average insertion time and force needed to insert the peg into different hole conditions

Tight holes and large angular misalignments required the manipulator to exert greater insertion forces; however, the additional time incurred was negligible. Heavily used holes required slightly more time due to the controller carefully matching the insertion force with the opposing reaction force to ensure stable engagement.

5.4 Stages of insertion

Table 5.3: Success rate and average time for each stage of the insertion process

Stage	**Success Rate**	**Average Time (s)**
Search	30/30	15
Adjustment	21/24	17.8
Insertion	24/30	23.7

5.5 Discussion

The experimental results demonstrate that the proposed tactile feedback-based control system enables robust, vision-free insertion across a wide range of real-world variations. Success rates remained high across uncertainties in hole location, orientation, and size. Moreover, the tactile sensor provided accurate pose feedback despite the lack of vision, validating the effectiveness of the centroid-based estimation method. Minor degradations in performance for extreme conditions (tight fits or large misalignments) were observed, which could be addressed in future work through adaptive grasping or learning-based compensation strategies.

Chapter 6

Conclusion

This chapter presented a comprehensive evaluation of the proposed control framework for vision-free peg-in-hole insertion using the Franka Emika Panda manipulator. Through a series of experiments, the system's robustness, accuracy, and efficiency were assessed under varying real-world uncertainties including positional displacements, angular misalignments, and hole condition variability.

The results demonstrated that the integration of tactile sensing and force-based control enabled reliable insertion without reliance on visual feedback. Success rates remained consistently high across most test conditions, particularly under moderate levels of uncertainty. The centroid-based pose estimation method using tactile feedback proved effective in guiding the manipulator during both the exploration and insertion phases.

Insertion time analysis revealed that while tight hole conditions and large misalignments increased the required force, their impact on task duration was minimal. Interestingly, heavily used holes, although mechanically more compliant, introduced slight delays due to the controller's cautious force balancing strategy.

Stage-wise analysis further confirmed the efficiency of the system, with nearly perfect performance in the *Search* phase and high success in the *Insertion* and *Adjustment* stages. These results affirm the potential of vision-free tactile-based insertion for practical applications, especially in unstructured or visually obstructed environments.

Future work could focus on extending the framework to dynamically adjust the grasp during insertion and incorporating learning-based approaches to improve performance under extreme uncertainty or complex geometries.

Bibliography

[1] S. Nagarajan and G. Perumaal, "Vision-based pose estimation of multiple robots for peg-in-hole assembly," *IEEE Transactions on Industrial Informatics*, vol. 14, no. 4, pp. 1722–1731, 2018.

[2] L. Berscheid, T. Schneider, and T. Kröger, "Tactile-based active inference for force-controlled peg-in-hole insertions," in *International Conference on Intelligent Robots and Systems (IROS)*. IEEE, 2023, pp. 1542–1549.

[3] S. Tang, M. Ding, and Y. Cheng, "Compare contact model-based control and contact model-free learning: A survey of robotic peg-in-hole assembly strategies," *IEEE Transactions on Robotics*, vol. 35, no. 2, pp. 346–362, 2019.

[4] T. Tang and H. Lin, "Autonomous alignment of peg and hole by force/torque feedback for robotic assembly," *2018 IEEE International Conference on Robotics and Automation (ICRA)*, pp. 1–6, 2018.

[5] J. Tremblay, D. Khaziev, and S. Birchfield, "Leveraging procedural generation for learning autonomous peg-in-hole assembly in space," *arXiv preprint arXiv:2405.01134*, 2024.

[6] P. Tonutti, M. Stankova, and F. Beltram, "Tacsl: A library for visuotactile sensor simulation and learning," *arXiv preprint arXiv:2408.06506*, 2024.

[7] T. Tang and H. Lin, "Teach industrial robots peg-hole insertion by human demonstration," *IEEE International Conference on Advanced Manufacturing*, pp. 201–208, 2018.

[8] K. Van Wyk, M. Culleton, J. Falco, and K. Kelly, "Comparative peg-in-hole testing of a force-based manipulation controlled robotic hand," *IEEE Transactions on Robotics*, vol. 34, no. 2, pp. 542–549, 2018.

[9] T. Lefebvre, J. Xiao, H. Bruyninckx, and G. De Gersem, "Active compliant motion: a survey," *Advanced Robotics*, vol. 19, no. 5, pp. 479–499, 2005.

[10] Z. Zhu and H. Hu, "Robot learning from demonstration in robotic assembly: A survey," *Robotics*, vol. 7, no. 2, p. 17, 2018.

[11] R. S. Sutton, A. G. Barto *et al.*, *Reinforcement learning: An introduction*. MIT press Cambridge, 1998, vol. 1, no. 1.

[12] T. Lefebvre, J. Xiao, H. Bruyninckx, and G. D. Gersem, "Active compliant motion: a survey," *Advanced Robotics*, vol. 19, no. 5, pp. 479–499, 2005.

[13] J. Su, R. Li, H. Qiao, J. Xu, Q. Ai, and J. Zhu, "Study on dual peg-in-hole insertion using of constraints formed in the environment," *Industrial Robot: An International Journal*, vol. 44, no. 6, pp. 730–740, 2017.

[14] T. Inoue, G. D. Magistris, A. Munawar, T. Yokoya, and R. Tachibana, "Deep reinforcement learning for high precision assembly tasks," in *2017 IEEE/RSJ International Conference on Intelligent Robots and Systems (IROS)*, Sept 2017, pp. 819–825.

[15] Y. Fan, J. Luo, and M. Tomizuka, "A learning framework for high precision industrial assembly," *CoRR*, vol. abs/1809.08548, 2018. [Online]. Available: http://arxiv.org/abs/1809.08548

[16] Z. Liu, Y. Xie, J. Xu, and K. Chen, "Laser tracker based robotic assembly system for large scale peg-hole parts," in *The 4th Annual IEEE International Conference on Cyber Technology in Automation, Control and Intelligent*, June 2014, pp. 574–578.

[17] Z. Qin, P. Wang, J. Sun, J. Lu, and H. Qiao, "Precise robotic assembly for large-scale objects based on automatic guidance and alignment," *IEEE Transactions on Instrumentation and Measurement*, vol. 65, no. 6, pp. 1398–1411, June 2016.

[18] A. Wan, J. Xu, H. Chen, S. Zhang, and K. Chen, "Optimal path planning and control of assembly robots for hard-measuring easy-deformation assemblies," *IEEE/ASME Transactions on Mechatronics*, vol. 22, no. 4, pp. 1600–1609, 2017.

[19] K. Zhang, J. Xu, H. Chen, J. Zhao, and K. Chen, "Jamming analysis and force control for flexible dual peg-in-hole assembly," *IEEE Transactions on Industrial Electronics*, vol. 66, no. 3, pp. 1930–1939, March 2019.

[20] J. Xu, Z. Hou, W. Wang, B. Xu, K. Zhang, and K. Chen, "Feedback deep deterministic policy gradient with fuzzy reward for robotic multiple peg-in-hole assembly tasks," *IEEE Transactions on Industrial Informatics*, pp. 1–1, 2018.

[21] Z. Hou, M. Philipp, K. Zhang, Y. Guan, K. Chen, and J. Xu, "The learning-based optimization algorithm for robotic dual peg-in-hole assembly," *Assembly Automation*, vol. 38, no. 4, pp. 369–375, 2018.

[22] D. E. Whitney, "Quasi-static assembly of compliantly supported rigid parts," *Journal of Dynamic Systems, Measurement, and Control*, vol. 104, no. 1, pp. 65–77, 1982.

[23] I. F. Jasim, P. W. Plapper, and H. Voos, "Contact-state modelling in force-controlled robotic peg-in-hole assembly processes of flexible objects using optimised gaussian mixtures," *Proceedings of the Institution of Mechanical Engineers, Part B: Journal of Engineering Manufacture*, vol. 231, no. 8, pp. 1448–1463, 2017.

[24] L. M. Brignone and M. Howarth, "A geometrically validated approach to autonomous robotic assembly," in *IEEE/RSJ International Conference on Intelligent Robots and Systems*, vol. 2, Sept 2002, pp. 1626–1631 vol.2.

[25] T. Tang, H.-C. Lin, Y. Zhao, W. Chen, and M. Tomizuka, "Autonomous alignment of peg and hole by force/torque measurement for robotic assembly," in *Automation Science and Engineering (CASE), 2016 IEEE International Conference on*. IEEE, 2016, pp. 162–167.

[26] B. D. Argall, S. Chernova, M. Veloso, and B. Browning, "A survey of robot learning from demonstration," *Robotics and autonomous systems*, vol. 57, no. 5, pp. 469–483, 2009.

[27] T. Tang, H.-C. Lin, and M. Tomizuka, "A learning-based framework for robot peg-hole-insertion," in *ASME 2015 Dynamic Systems and Control Conference*. American Society of Mechanical Engineers, 2015, pp. V002T27A002–V002T27A002.

[28] T. Tang, H.-C. Lin, Y. Zhao, Y. Fan, W. Chen, and M. Tomizuka, "Teach industrial robots peg-hole-insertion by human demonstration," in *Advanced Intelligent Mechatronics (AIM), 2016 IEEE International Conference on*. IEEE, 2016, pp. 488–494.

[29] R. S. Sutton and A. G. Barto, *Reinforcement learning: An introduction*. MIT press, 2018.

[30] Z. Zhu and H. Hu, "Robot learning from demonstration in robotic assembly: A survey," *Robotics*, vol. 7, no. 2, p. 17, 2018.

[31] M. Kyrarini, M. A. Haseeb, D. Ristic-Durrant, and A. Gräser, "Robot learning of industrial assembly task via human demonstrations," *Autonomous Robots*, pp. 1–19, 2018.

[32] J. Kober, J. A. Bagnell, and J. Peters, "Reinforcement learning in robotics: A survey," *The International Journal of Robotics Research*, vol. 32, no. 11, pp. 1238–1274, 2013.

[33] S. Levine, N. Wagener, and P. Abbeel, "Learning contact-rich manipulation skills with guided policy search," in *Robotics and Automation (ICRA), 2015 IEEE International Conference on*. IEEE, 2015, pp. 156–163.

[34] J. Luo, E. Solowjow, C. Wen, J. A. Ojea, and A. M. Agogino, "Deep reinforcement learning for robotic assembly of mixed deformable and rigid objects," in *2018 IEEE/RSJ International Conference on Intelligent Robots and Systems (IROS)*, Oct 2018, pp. 2062–2069.

[35] G. Thomas, M. Chien, A. Tamar, J. A. Ojea, and P. Abbeel, "Learning robotic assembly from cad," *CoRR*, vol. abs/1803.07635, 2018. [Online]. Available: http://arxiv.org/abs/1803.07635

[36] A. S. Polydoros and L. Nalpantidis, "Survey of model-based reinforcement learning: Applications on robotics," *Journal of Intelligent & Robotic Systems*, vol. 86, no. 2, pp. 153–173, 2017.

[37] W. Newman, Y. Zhao, and Y.-H. Pao, "Interpretation of force and moment signals for compliant peg-in-hole assembly," vol. 1, pp. 571–576, 2001.

[38] J. Oh and J.-H. Oh, "A modified perturbation/correlation method for force-guided assembly," *Journal of Mechanical Science and Technology*, vol. 29, 2001.

[39] H.-C. Song, Y.-L. Kim, and J.-B. Song, "Guidance algorithm for complex-shape peg-in-hole strategy based on geometrical information and force control," *Advanced Robotics*, vol. 30, no. 8, pp. 552–563, 2016.

[40] H. Qiao and S. Tso, "Three-step precise robotic peg-hole insertion operation with symmetric regular polyhedral objects," *International Journal of Production Research*, vol. 37, no. 15, pp. 3541–3563, 1999.

[41] "Hole detection algorithm for chamferless square peg-in-hole based on shape recognition using f/t sensor," *International Journal of Precision Engineering and Manufacturing*, vol. 15, pp. 425–432, 2014.

[42] J. Jiang, Z. Huang, Z. Bi, X. Ma, and G. Yu, "State-of-the-art control strategies for robotic pih assembly," vol. 65, 2020, p. 101894.

[43] "Intuitive peg-in-hole assembly strategy with a compliant manipulator," in *2013 44th International Symposium on Robotics, ISR 2013*, 2013.

[44] "Compliance-based robotic peg-in-hole assembly strategy without force feedback," *IEEE Transactions on Industrial Electronics*, vol. 64, pp. 6299–6309, 2017.

[45] T. Zhang, X. Liang, and Y. Zou, "Robot peg-in-hole assembly based on contact force estimation compensated by convolutional neural network," *Control Engineering Practice*, vol. 120, p. 105012, 2022.

[46] S. Kim and A. Rodriguez, "Active extrinsic contact sensing: Application to general peg-in-hole insertion," 2021.

[47] "Comparative peg-in-hole testing of a force-based manipulation controlled robotic hand," *IEEE Transactions on Robotics*, vol. 34, pp. 542–549, 2018.

[48] J. Bimbo, S. Luo, K. Althoefer, and H. Liu, "In-hand object pose estimation using covariance-based tactile to geometry matching," *IEEE Robotics and Automation Letters*, vol. 1, no. 1, pp. 570–577, 2016.

[49] S. Dikhale, K. Patel, D. Dhingra, I. Naramura, A. Hayashi, S. Iba, and N. Jamali, "Visuotactile 6d pose estimation of an in-hand object using vision and tactile sensor data," *IEEE Robotics and Automation Letters*, vol. 7, no. 2, pp. 2148–2155, 2022.

[50] A. Albini, F. Grella, P. Maiolino, and G. Cannata, "Exploiting distributed tactile sensors to drive a robot arm through obstacles," *IEEE Robotics and Automation Letters*, vol. 6, pp. 4361–4368, 2021.

[51] D. Ma, S. Dong, and A. Rodriguez, "Extrinsic contact sensing with relative-motion tracking from distributed tactile measurements," in *2021 IEEE International Conference on Robotics and Automation (ICRA)*. IEEE, 2021, pp. 11 262–11 268.

[52] Y. Fan *et al.*, "Vision-based hybrid force control for peg-in-hole assembly," *IEEE Transactions on Robotics*, vol. 38, no. 4, pp. 2120–2135, 2022.

[53] J. Huang *et al.*, "Multi-modal learning for adaptive peg-in-hole assembly," *IEEE Robotics and Automation Letters*, vol. 6, no. 3, pp. 4902–4909, 2021.

[54] J. Zhang *et al.*, "Vision-tactile fusion for contact-rich manipulation," *International Journal of Robotics Research*, vol. 42, pp. 320–337, 2023.

[55] B. Ward-Cherrier *et al.*, "The tactip family: Soft optical tactile sensors with 3d-printed biomimetic morphologies," *Soft Robotics*, vol. 5, no. 2, pp. 216–227, 2018.

[56] S. Kim and A. Rodriguez, "Active extrinsic contact sensing: Application to general peg-in-hole insertion," in *2022 International Conference on Robotics and Automation (ICRA)*. IEEE, 2022, pp. 10 241–10 247.